High-resolution spectroscopy of light hypernuclei with the decay-pion spectroscopy
(A letter of intent)

S. Nagao (contact person),
F. Garibaldi, T. Gogami, P. Markowitz, S.N. Nakamura, B. Pandy, J. Reinhold,
L. Tang, G.M. Urciuoli
on behalf of JLab Hypernuclear Collaboration

Abstract

Λ binding energy represents one of the most fundamental values to describe ΛN interaction and Λ hypernuclear structures. We propose to study s and p-shell Λ hypernuclei using decay pion spectroscopy. We aim to newly determine the Λ binding energies of several light hypernuclei with an accuracy of ∼10 keV, which is the world's best accuracy. The renovated binding energies investigate ΛN interaction, neutron-rich hypernuclei, hypertriton puzzle, and hypernuclear spin-parity state. The proposed experiment uses Enge as a pion spectrometer and the K^+ tagger HKS. The experiment can take data parallel with the other proposed $(e, e'K^+)$ experiments (E12-15-008, E12-20-013). We request 336 hours of beamtime for specialized setup with a C target in the proposed experiment.

1 Introduction

1.1 Hypernuclei

The Λ hypernucleus is one of the exotic nuclei which contains Λ particles. The binding energies of Λ hypernuclei give one of important information on the ΛN interaction. The binding energy of Λ of a hypernucleus is defined by

$$B_\Lambda = M_{core} + M_\Lambda - M_{HYP}, \tag{1}$$

where the mass M_{core} is the mass of the core nucleus, which is the nucleus after removing Λ from the hypernucleus. M_Λ and M_{HYP} are the masses of the Λ and the hypernucleus, respectively. About 40 species of hypernuclei, from the lightest hypernuclei ${}^{3}_{\Lambda}$H to the heaviest ${}^{209}_{\Lambda}$Bi, have been observed, and most of the light hypernuclei were observed by emulsion experiments in the 1960s to 70s. The statistical uncertainties of the measurements are a several-tenth keV to a few hundred keV. Figure 1 shows a hypernuclear chart up to observed p-shell hypernuclei together with Λ binding energies and statistical uncertainties as a MeV unit. Triangles at the edge of boxes mean the experimental methods for determining the Λ binding energies.

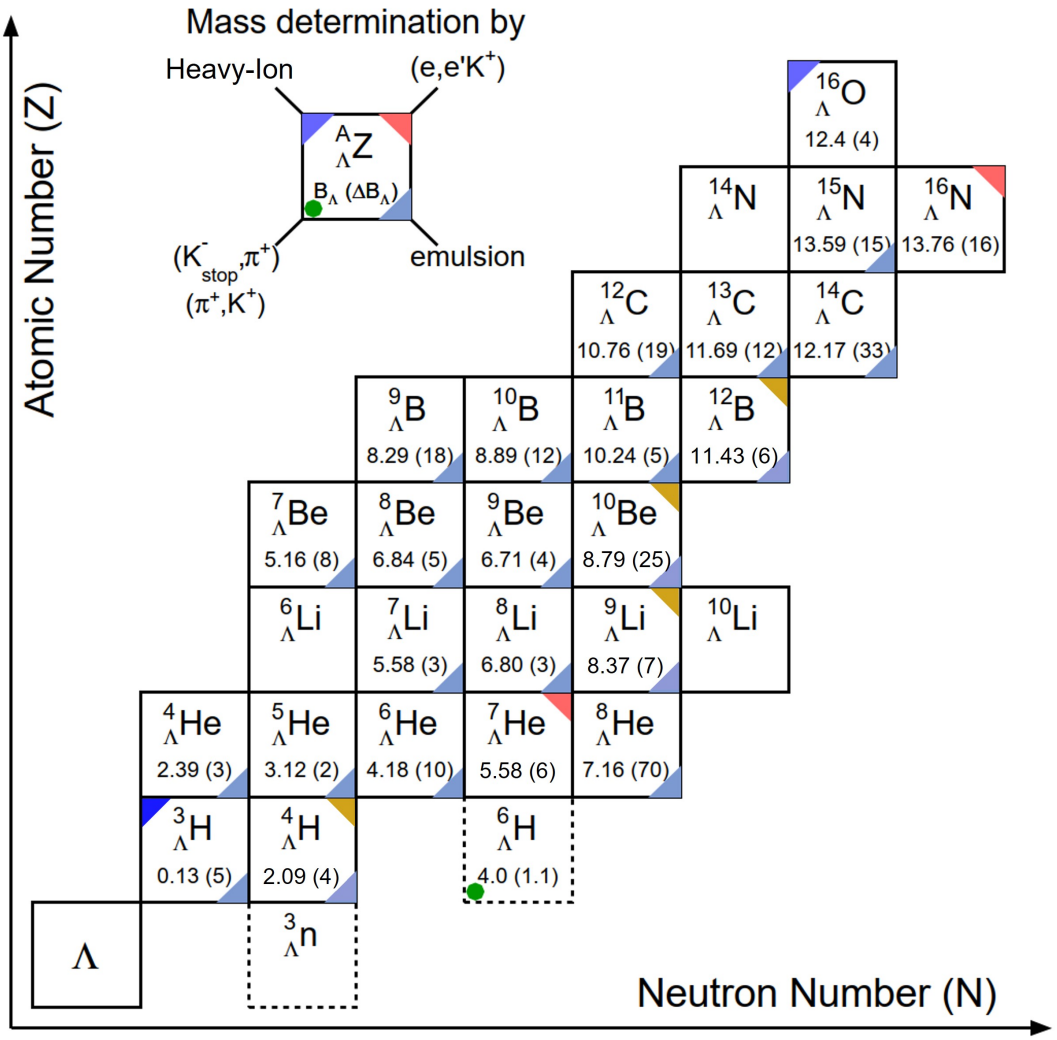

Figure 1: A Λ hypernuclear chart. The Λ binding energies are refered by the hypernuclear database [1] The existences are not well confirmed for hypernuclei in dashed boxes ($^{3}_{\Lambda}$n and $^{6}_{\Lambda}$H) [2, 3]

.

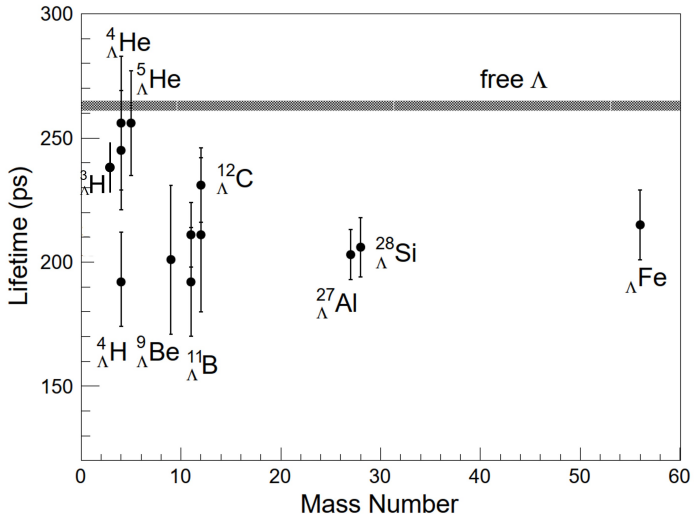

Figure 2: Lifetimes of hypernuclei. The lifetime of a Λ in free space is shown as a black band. The lifetimes of hypernuclei are given by the hypernuclear database [1].

The lifetimes of the hypernuclear ground states are about 200 ps from the light to the medium-heavy mass region, a lifetime similar to Λ in the free space (Figure 2). Hypernuclei have two weak-decay modes: mesonic weak decay (MWD), in which hypernuclei emit pions, and non-mesonic weak decay (NMWD), in which they do not emit pions. MWD is a similar decay mode to the free Λ decay, such as $\Lambda \to p + \pi^-$, which is the primary decay mode on the *s*-shell hypernuclei. NMWD is a unique decay mode in the hypernuclear medium through interactions between Λ and nucleons such as Λ+N→N+N, the dominant decay mode on the heavy mass hypernuclei. The total decay widths are expressed as:

$$\Gamma_{tot} = \Gamma_{\pi^-} + \Gamma_{\pi^0} + \Gamma_{nm}, \tag{2}$$

where Γ_{π^-}, Γ_{π^0}, and Γ_{nm} are the decay width of π^- emission, π^0 emission, and NMWD, respectively.

Figure 3 shows experimental results and a theoretical calculation by Motoba for the *p*-shell hypernuclei. The MWD branch is well understood in the theoretical framework because the uncertainty of the weak decay coupling constant is small. The theoretical results successfully reproduced the experimental results well. Though the π^- decay widths of light hypernuclei are several times smaller than the total decay width of a free Λ, MWD is still in significant decay mode. The decay width becomes larger in the neutron-rich hypernuclei. $\Gamma_{\pi^-}/\Gamma_\Lambda$ is 0.397 and 0.356 for $^{8}_{\Lambda}$Li and $^{12}_{\Lambda}$B, respectively.

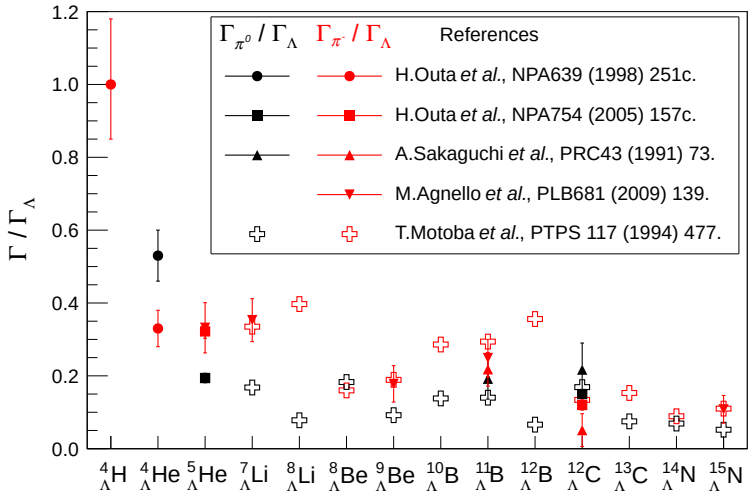

Figure 3: Decay width of light hypernuclear mesonic weak decay. Black points mean the mesonic weak decay widths with π^0 emission normalized with the free Λ decay width, and red points mean with π^- emission.

1.2 Mass Spectroscopic Techniques

The hypernuclear spectroscopy with the $(e, e'K^+)$ reaction was established at JLab [4, 5]. In this experiment, two high-momentum resolution spectrometers were operated to measure the momenta of scattered electrons and generated K^+s with a relative momentum resolution of $\Delta p/p = 10^{-4}$, and the masses of hypernuclei were deduced using the missing mass method. Thanks to the high intensity and the high-resolution primary electron beam, the $(e, e'K^+)$ reaction spectroscopy can observe hypernuclear peaks with a good resolution ($\sim$0.5 MeV in FWHM). In addition, determination of the absolute Λ binding energy with an accuracy of a few hundred keV is possible thanks to good calibration sources of Λ and Σ^0 masses produced with the $p(e, e'K^+)$Y reactions. Figure 4 shows the $^{12}_{\Lambda}$B mass spectrum in JLab E05-115. Clear hypernuclear ground state and excited peaks were successfully observed with an accuracy of $\sim$100 keV.

The $(e, e'K^+)$ reaction spectroscopy is a powerful tool for discussing a hypernuclear structure and energy levels in the 100 keV precision. However, this precision is insufficient to resolve the problems in the light hypernuclear region, such as the Charge Symmetry Breaking effect in the ΛN interaction, ΛN-ΣN coupling effect, and the hypertriton puzzle. Because the hypernuclear Λ binding energy can predict very precisely, especially for the light mass region thanks to the recent progress of theoretical frameworks such as the few-body calculation with the Gaussian Expansion Method and the Effective Field Theory, much more accurate hypernuclear mass spectroscopy is essential.

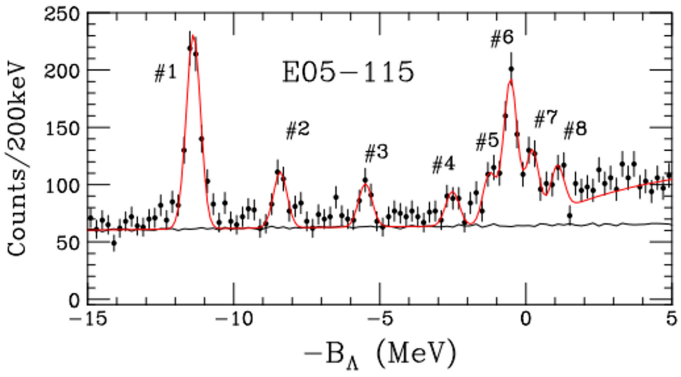

Figure 4: $^{12}_{\Lambda}$B mass spectrum of E05-115 at JLab Hall-C [6].

2 Physics Motivation

2.1 Study of the ΛN Interaction

Measurement of the ΛN interaction with the scattering experiment is much more difficult than that of the NN interaction due to the short lifetime of Λ particle. One can expect the interaction from the limited Λp scattering and hypernuclear data. Since there are no Λn scattering data, hypernuclear frameworks have assumed the charge Symmetry. However, recent results of the hypernuclear γ-ray spectroscopy and the decay pion spectroscopy confirmed the significant ΛN Charge Symmetry Breaking (CSB) effect for the A=4 system [7, 8]. On the other hand, the significant breaking cannot be observed for the A=7 system [9, 10]. Because the breaking effect would appear with a few 100 keV in the calculation and the experimental uncertainties are similar, a much more accurate measurement about a few tens keV is necessary to resolve the CSB effect quantitatively.

2.2 Study of neutron-rich Λ Hypernuclei

One of the reasons why the significant CSB effect appears in the iso-doublet hypernuclei is advocated to be a mixing effect of Σ particles from the ΛΣ conversion [11]. The mass difference between Λ and Σ is about 80 MeV/c^2, much smaller than that of NΔ (∼300 MeV/c^2). Therefore, the admixture probability of a virtual Σ particle is not negligible in a hypernucleus (∼2%) [12]. The Σ effect appears as a ΛN-ΣN coupling effect which is a non-negligible effect explaining Λ binding energy for many hypernuclei simultaneously. Precise data of Λ binding energies for neutron-rich hypernuclei would be critical inputs evaluating the strength of ΛN-ΣN coupling effect because the neutron-rich hypernuclear core has a large iso-spin. The reaction spectroscopy, such as the (π^+, K^+) and the $(e, e'K^+)$ reactions, can only produce Λ hypernuclei with β-stability region (Z∼N). The different approaches and the precise measurement of neutron-rich hypernuclei are essential subjects.

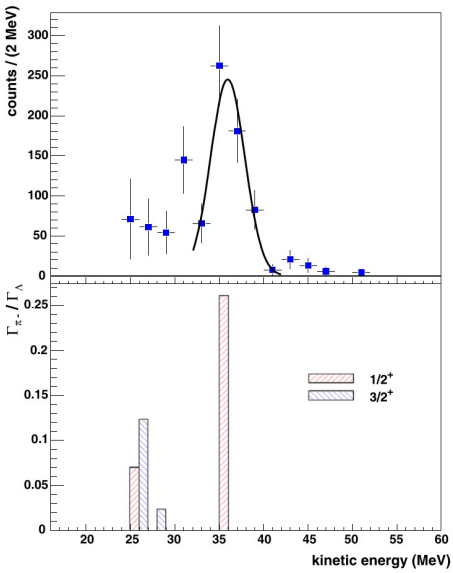

Figure 5: Kinetic energy spectra of MWD π^- from ${}^{7}_{\Lambda}$Li [20]. Experimental result by FINUDA (Top). Theoretical prediction (Bottom).

2.3 Hypertriton Puzzle

Hypertriton is the lightest and simplest hypernuclei, which is one of most important input to investigate hypernuclear frameworks. Bubble chamber and emulsion had measured the hypertriton binding energy and lifetime as a very shallow Λ binding energy ($B_\Lambda = 0.13 \pm 0.05(stat.)$ MeV) and a long lifetime hypernucleus in 1960s [13, 14]. However, some recent results by the heavy-ion experiments surprise suggest a completely different picture, namely a much deeper bound state ($B_\Lambda = 0.41 \pm 0.12(stat.) \pm 0.11(syst.)$ MeV) and a much shorter lifetime [2, 15, 16, 17]. On the other hand, resolving the hypertriton puzzle needs more accurate data to discuss the hypertriton picture. As additional experiments have been taking data or planning, the hypertriton is one of the most hot research subject.

2.4 Spin-Parity Determination

The decay pion spectra have information on the spin-parity of the initial hypernuclear ground state because the decay mode has a selectivity of the initial hypernuclear and the final daughter nucleus spin-parity state. Due to the experimental difficulties, most hypernuclei are not identified in their spin-parity state. However, some theoretical calculations have predicted the expected spectra by changing the hypernuclear spin-parity state [18, 19]. The prediction were confirmed, and the spin-parities of some hypernuclei were determined with the (K^-_{stop}, π^-) reaction at FINUDA [20]. Figure 5 shows the decay pion spectrum by the FINUDA experiment and the theoretical prediction of $1/2^+$ and $3/2^+$ states. The spectra support $1/2^+$ state as a ground state of ${}^{7}_{\Lambda}$Li.

2.5 Goal of the proposed experiment

The decay pion spectroscopy started and has been developed to resolve the above issues in the light hypernuclei at Mainz Microtron (MAMI) in Germany. The experiment successfully measured the Λ binding energy of ${}^{4}_{\Lambda}\mathrm{H}$ with a precision of $\sim$10 keV: the precision is the world's best. However, it was difficult to observe other hypernuclei due to the limited hypernuclear yield and the spectrometer performance. We want to propose a new decay pion spectroscopy with high statistics as a parallel experiment of the $(e, e'K^+)$ experiment. The experiment would newly determine the Λ binding energies for several hypernuclei with the world's highest accuracy ($\sim$10 keV) and give significantly impact hypernuclear physics.

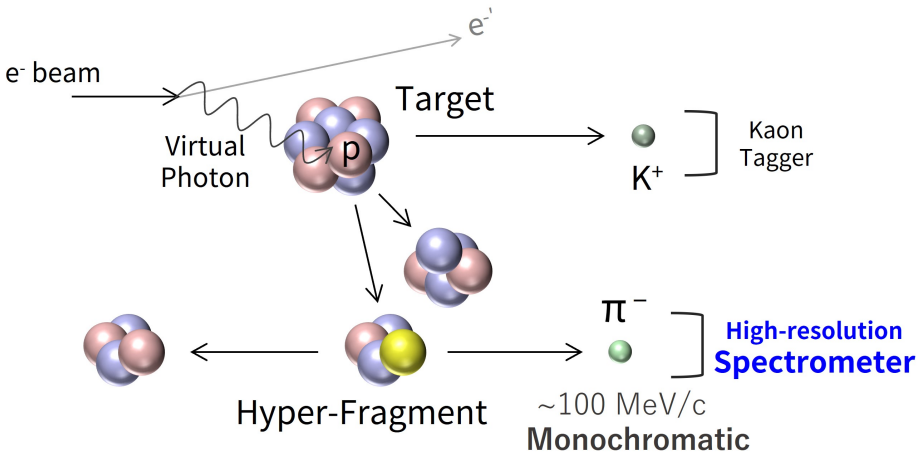

Figure 6: A schematic drawing of the hypernuclear decay pion spectroscopy.

3 Decay pion spectroscopy

Figure 6 shows a schematic drawing of this experimental principle. In this experiment, masses of hypernuclei M_{HYP} are deduced by measuring a monochromatic momentum of a pion from a two-body decay of a hypernucleus stopped in the target as follows,

$$M_{HYP} = \sqrt{M_{nucl}^2 + p_{\pi^-}^2} + \sqrt{M_{\pi^-}^2 + p_{\pi^-}^2}. \tag{3}$$

The momentum of the decay pion that we measure is represented as p_{π^-}. M_{nucl} and M_{π^-} are a mass of the daughter nucleus and a mass of π^-, respectively, known quantities. For example, the masses of ^{4}He and π^-, daughter particles of mesonic weak decay in $^4_\Lambda$H, are determined with an accuracy of 0.06 eV [21] and 0.35 keV [22], respectively.

The Λ binding energy of a hypernucleus (B_Λ) can be obtained as Eq.(1). Since these masses are also well known, for example, a mass of ^{3}H (core nucleus of $^4_\Lambda$H) is 2808.9210045(23) MeV [21], the Λ binding energy can be deduced only by measuring the momentum of hypernuclear decay pion.

In the $(e, e'K^+)$ missing mass spectroscopy, the momenta of scattered electrons ($\sim$1 GeV/c) and those of K^+s ($\sim$1 GeV/c) are measured in two spectrometers with a relative momentum resolution of $\Delta p/p \sim 10^{-4}$. The energy resolution on the final spectrum is a quadratic sum of the momentum resolution for the beam, the scattered electron, and the K^+. On the other hand, in the hypernuclear decay pion spectroscopy, the binding energies of hypernuclei can measure with an energy resolution of $\sim$10 keV because the mass can be deduced from the relatively lower momentum pion only. Thus, this method can obtain extreme mass resolution and best mass spectroscopy for the ground state energies of light Λ hypernuclei.

The method needs to tag K^+ suppressing background π^-s from non-strangeness production. The performance of K^+ identification is essential to suppress the background height on the final spectrum. Measurements of the scattered electrons are not necessary.

Hypernuclei are produced using the $^AZ(\gamma, K^+)X$ reaction from the electron beams. In

Table 1: A list of expected decay pion momenta.

Hypernuclei	Decay mode	p_{π^-} (MeV/c)
${}^{3}_{\Lambda}$H	^{3}He + π^-	114.4
${}^{4}_{\Lambda}$H	^{4}He + π^-	133.0
${}^{6}_{\Lambda}$H	^{6}He + π^-	135.3
${}^{7}_{\Lambda}$He	^{7}Li + π^-	114.8
${}^{7}_{\Lambda}$Li	^{7}Be + π^-	108.1
${}^{8}_{\Lambda}$He	^{8}Li + π^-	116.5
${}^{8}_{\Lambda}$Li	2α + π^-	124.2
${}^{8}_{\Lambda}$Be	^{8}B + π^-	97.2
${}^{9}_{\Lambda}$Li	^{9}Be + π^-	121.3
${}^{9}_{\Lambda}$B	^{9}C + π^-	96.8
${}^{10}_{\Lambda}$B	^{10}C + π^-	100.5
${}^{11}_{\Lambda}$B	^{11}C + π^-	86.5
${}^{12}_{\Lambda}$B	^{12}C + π^-	115.9
${}^{12}_{\Lambda}$C	^{12}N + π^-	91.5
${}^{13}_{\Lambda}$C	^{13}N + π^-	92.3
${}^{14}_{\Lambda}$C	^{14}N + π^-	101.2
${}^{15}_{\Lambda}$N	^{15}O + π^-	98.4
${}^{16}_{\Lambda}$N	^{16}O + π^-	106.2

this method, observable hypernuclei are not only a directly produced hypernucleus (${}^{A}_{\Lambda}(Z-1)$) but also hyper-fragments; they are fragmented hypernuclei produced with breakups of the nucleus due to recoil momentum transfer in the reaction.

Table 1 summarizes observable hypernuclei and expected momentum calculated by the literature binding energies. A parent hypernucleus of a decay pion peak can be identified by its momenta because each hypernucleus has a unique pion momentum. Horizontal bars mean the possible hypernuclear limit in each target. ${}^{3}_{\Lambda}$H and ${}^{4}_{\Lambda}$H, above the first bar, would be produced by a ^{6}Li target. Hypernuclei above the second bar are by a ^{7}Li target. Hypernuclei above the third, fourth, and last are by a ^{9}Be, a ^{12}C, and a ^{16}O target, respectively.

The primary background source of the experiment is π^- from Quasi-Free hyperons such as $\Lambda \to p + \pi^-$. Monte-Carlo simulation assumed by the target nuclear Fermi-Motion and the elemental cross-section of the N(γ, K^+)Y reactions can work to estimate the expected distribution and amount of the π^- background (Figure 7). Since SAPHIR and CLAS have precisely measured the elemental cross-section, reliable simulation is possible. Though a decay pion momentum from a free Λ is 101 MeV/c, the pion momentum is smaller (about 70 MeVc) at $\theta_\pi \sim 135$ deg because of the Lorentz boost. The most significant background, the decay pion from the quasi-free Λ, does not overlap with the hypernuclear decay pions. Although a decay pion from $\Sigma^- \to n + \pi^-$ would overlap with the decay pion peaks from hypernuclei, the amount of the background is relatively small.

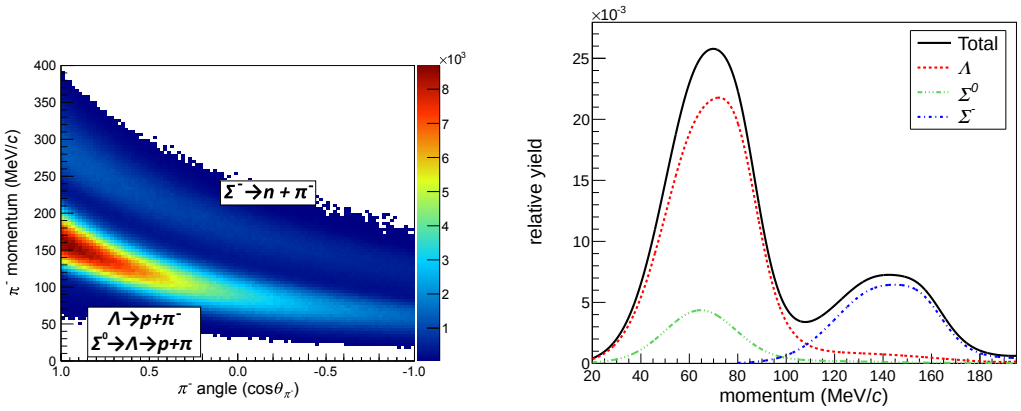

(a) 2D plot

(b) $\cos\theta_\pi = -0.7$

Figure 7: Expected distribution of quasi-free hyperon backgrounds. (a) 2D-plot of momentum and angular distribution. (b) Momentum projection at $\cos\theta_\pi = -0.7$.

3.1 Previous Study at MAMI

MAMI-C is a continuous electron accelerator at Mainz University in Germany. With the four-stage Microtrons, MAMI-C can accelerate electrons up to 1508 MeV, which is enough energy to produce $s\bar{s}$ quarks. The electron beam is available in the A1 experimental Hall (Figure 8). The Hall consists of an electron beam line, targets, and surrounding spectrometers (Spek-A, Spek-B, Spek-C, and Kaos). In the 2012 and 2014 experiments, Spek-A and Spek-C, which are well-established high-resolution spectrometers ($\Delta p/p \sim 10^{-4}$) were used as decay pion spectrometers. Kaos with a short orbit spectrometer (~6 m) was operated as a K^+ tagger. The production target (^{9}Be foil, 0.125 mm) was tilted at 54 deg to the electron beam to get higher hypernuclear yield by suppressing the energy-struggling effect of the decay pions.

Figure 9 shows the observed pion momentum distribution in 2012. The decay pion from $^4_\Lambda$H was clearly observed at $p_\pi = 132.92\pm0.02$ MeV/c, which corresponds to $B_\Lambda = 2.12\pm0.01$ MeV. The peak resolution was 0.15 MeV/c in FWHM, which was improved to 0.07 MeV/c in the 2014 experiment thanks to improvements of the spectrometer vacuum extension. The number of decay pions from $^4_\Lambda$H was 37 counts, which corresponds to a ~1% formation probability of Λ production. The probability is 40% less than the $(K^-_{stop}, \pi-)$ result [23] due to the 40% larger Λ momentum transfer than the $(K^-_{stop}, \pi-)$ reaction. Thus, the decay pion spectroscopy was successfully performed at MAMI, and an updated experiment with a Li target was also done in 2022.

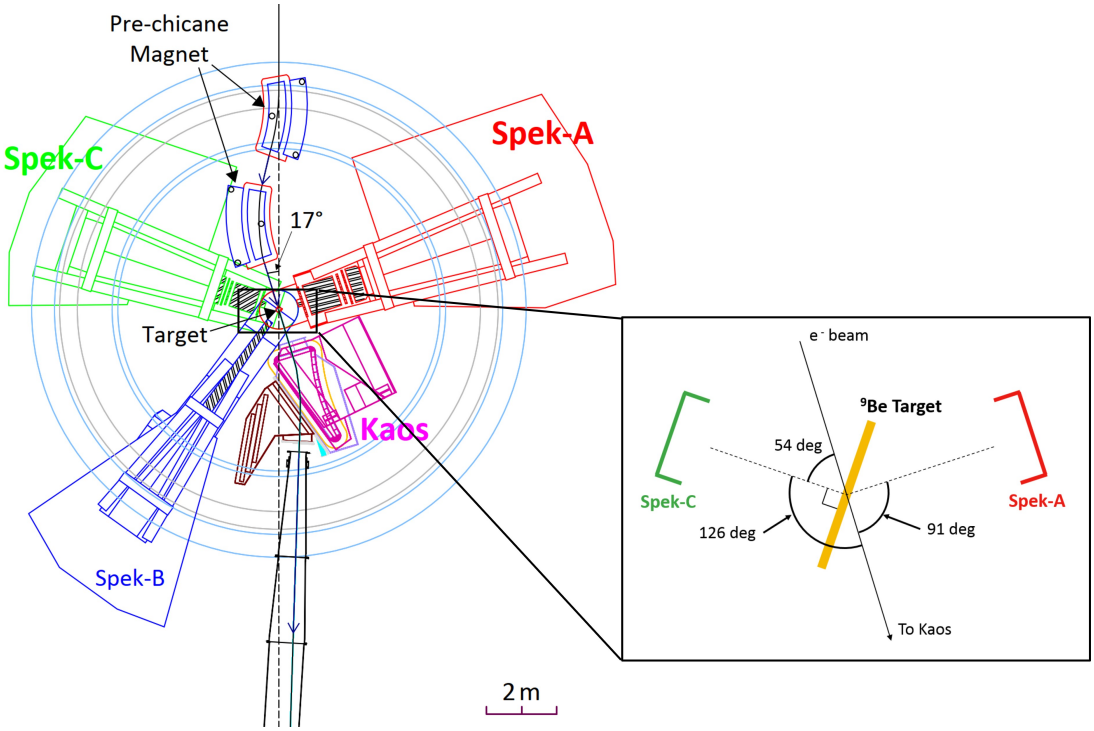

Figure 8: Top view of the decay pion spectroscopy experiment at MAMI A1 Hall

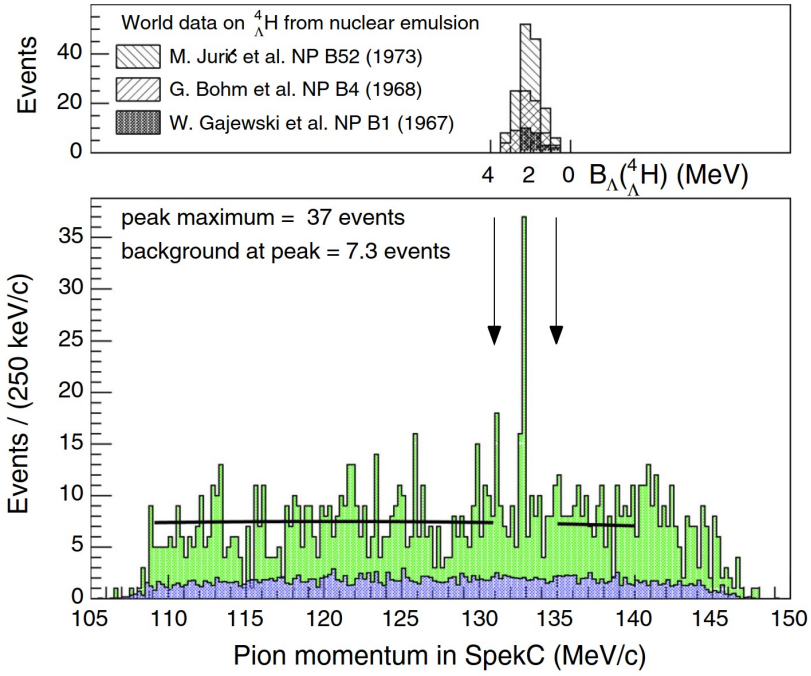

Figure 9: Pion momentum distribution of the MAMI experiment.

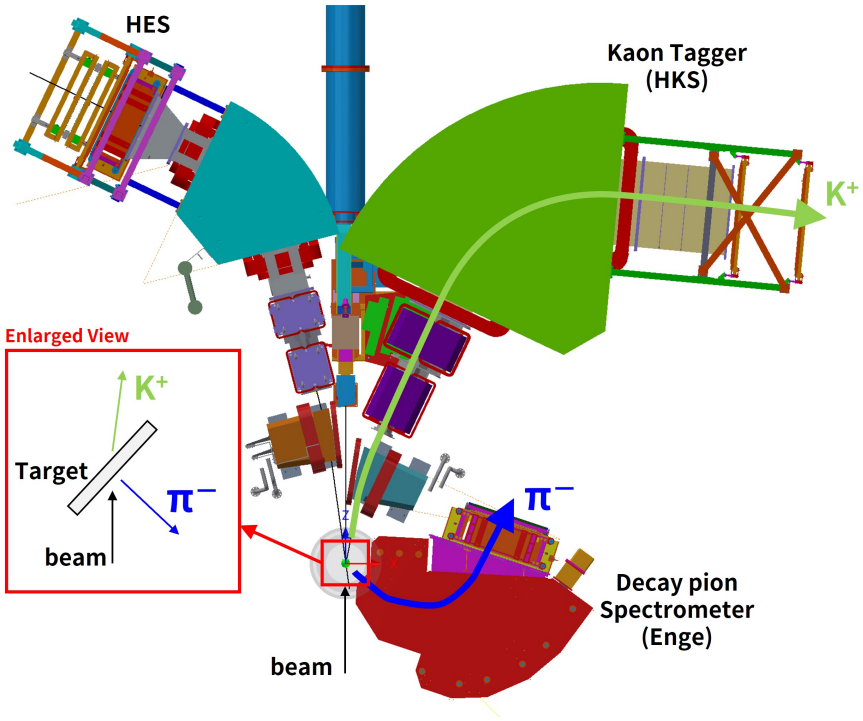

Figure 10: Overview of the proposed experimental setup

4 Proposed Experiment

The MAMI experiment was successfully observed the ${}^{4}_{\Lambda}$H peak. On the other hand, the following hypernuclear peaks are not observed due to the limited yield and large background. Since the decay pion yields from the other hypernuclei are expected to be ten times more minor, yield and background suppression improvements are essential. However, the large updates are problematic due to the limitations of K^+ tagger performance, the radiation levels, and the DAQ system at MAMI. If the decay pion spectroscopic method is applied to JLab, significant improvement would be possible because better Λ production yield and better K^+ identification are possible. When hypernuclear masses are successfully brought with an accuracy of 10 keV or less, discussions associated with light hypernuclei, such as the CSB effect, is innovated. Only decay pion spectroscopy can achieve such an accurate measurement. Therefore, we would like to propose the decay pion experiment at JLab as a parallel experiment with the $(e, e'K^+)$ experiments.

4.1 Experimental Setup

Figure 10 shows the experimental setup. The proposed experiment will install a third spectrometer (Enge magnet) as a pion spectrometer in addition to the K^+ spectrometer (HKS) and the scattered electron spectrometer (HES), which will be used for the $(e, e'K^+)$ experiments. The Enge magnet is installed at the backward angles (135 deg) for the electron beam to suppress background π^-s from quasi-free hyperons.

4.1.1 Enge spectrometer

The previous hypernuclear experiments at JLab (E89-008 and E01-011) had used the Enge magnet. Enge is a split-pole magnet, designed as a hardware spectrometer. The weight of the magnet is 54 tons. When one uses the Enge magnet as a hardware spectrometer, the focal plane shape has excellent linearity to the particle momentum, as shown in Figure 11. The central-ray of a particle trajectory will be set 110 MeV/c to cover a full acceptance of decay pion candidates. A power supply (140 A / 36 V) and cooling water (5 L/min, 15 PSI), which are small, are necessary to operate the magnet. The momentum dispersion is $< p|x > 1.4$ cm/%. The expected momentum resolution and solid angles are $\Delta p/p = 3 \times 10^{-4}$ and 4 msr, respectively from a Geant4 Monte-Carlo simulation.

The detector hut will consist of a focal plane (FP) detector, a drift chamber, and scintillation (TOF) counters.

The FP detector locates in a vacuum and consists of scintillation fiber detectors with a diameter of 0.75 mm. The hit position of the FP detector represents the pion momentum. α-sources installed at the target position work as a momentum calibration source. Table 2 listed α-source what we are planning to use as calibration sources. As typical α-source ^{241}Am emits $E = 5.48556(12)$ MeV α particle, which corresponds to 101.1479(11) MeV/c/q and matches to the decay pion momenta, the momentum of Enge can calibrate with an accuracy of less than 10 keV/c. The calibration will be performed before the beamtime and beam maintenance period.

Another tracking device drift chamber is necessary to measure the flight path length from the target to the focal plane. 2-layer TOF counters, which have ∼100 ps time resolution in rms, determine the trigger and hit timing. As much better timing resolution (a few 100 ps in rms) of the conscience time between a decay pion and an associated K^+ is achievable than that in the MAMI experiments by using the above two detectors and HKS detectors, much better PID performance and accidental background suppression power are achievable in the proposed experiment.

Targets that are the same as the proposed $(e, e'K^+)$ experiments (E12-15-008 and LoI) tilted 50 degrees are used for the hypernuclear production target, as shown in Table 3. Although the main production targets are Li, Be, B, and C, there is a chance to observe unexpected decay pion peaks from p and sd-shell hypernuclei with Al and Ca targets. Parallel data taking is possible with the proposed $(e, e'K^+)$ experiments when the trigger is defined by,

$$(HKS \wedge HES) \vee (HKS \wedge Enge). \tag{4}$$

Maximum physics outputs are available without long additional beamtime requests.

4.1.2 Advantage

There are several advantages of the decay pion spectroscopy at JLab compared to the MAMI experiment.

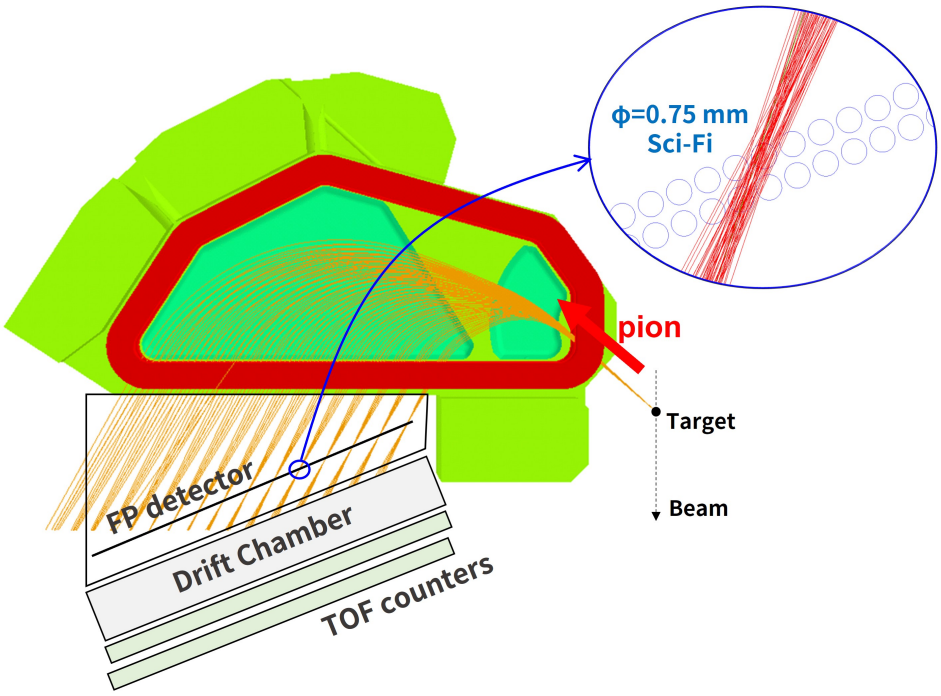

Figure 11: Enge magnet and detector setup plan. Particle tracks which are generated from the target with a momentum range of $\delta p = -40 \sim 110\%$ every 10% momentum bite are shown in the orange lines.

Table 2: List of α-sources.

Nuclide	Typical Energy (MeV)	Momentum (MeV/c/q)
^{148}Gd	3.128787(24)	77.03415(29)
^{237}Np	4.7710(15), 4.7880(15)	94.326(15), 94.494(15)
^{241}Am	5.44280(13), 5.48556(12)	100.7526(12), 101.1479(11)
^{244}Cm	5.76270(3), 5.80482(5)	103.6734(3), 104.0519(4)

Table 3: Target list.

Target	Thickness (mm)	Thickness (mg/cm^2)	Hypernuclei
^{6}Li	2.8	150	$^{3,4}_{\Lambda}$H
^{9}Be	0.8	150	$^{3,4,6}_{\Lambda}$H, $^{7,8}_{\Lambda}$He, $^{7,8,9}_{\Lambda}$Li, $^{8}_{\Lambda}$Be
^{11}B	0.7	150	$^{3,4,6}_{\Lambda}$H, $^{7,8}_{\Lambda}$He, $^{7,8,9}_{\Lambda}$Li, $^{8}_{\Lambda}$Be
^{12}C	0.9	150	$^{3,4,6}_{\Lambda}$H, $^{7,8}_{\Lambda}$He, $^{7,8,9}_{\Lambda}$Li, $^{8}_{\Lambda}$Be, $^{9,10,11,12}_{\Lambda}$B
^{27}Al	0.6	150	s, p, sd-shell hypernuclei?
^{40,48}Ca	1.0	150	s, p, sd-shell hypernuclei?
^{208}Pb	0.13	150	s, p, sd-shell hypernuclei?

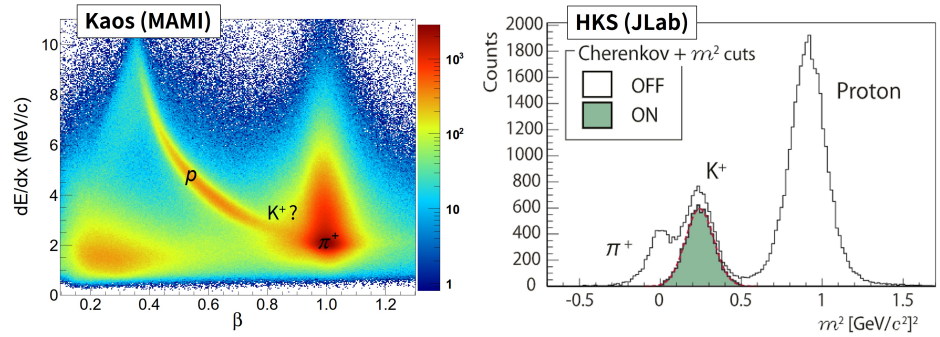

Figure 12: K^+ ID performance. A correlation of the energy deposit and particle velocity β measured by the TOF counters of Kaos at MAMI (Left). A mass square distribution calculated by β and the momentum with HKS at JLab E05-115 [5] (Right).

- Effective K^+ identification
  The Kaos spectrometer's particle ID performance at MAMI is insufficient to select K^+ clearly. Figure 12 shows the K^+ ID plot of Kaos and HKS. Kaos has the TOF counters with a typical flight path length of 1 m and only the two layers of Aerogel Cherenkov detectors. The huge π^+ background made finding K^+ from the PID plot difficult. HKS at JLab consists of the TOF counters with the 1.5 m flight path length, triple layers of the Aerogel Cherenkov detectors, and the double layers of water Cherenkov detectors. After applying Cherenkov cuts, K^+ can identify the mass-square distribution calculated by the TOF and the momentum.

- Better coincidence time selection
  Figure 13 shows the coincidence time spectra of "Kaos and Spek-C" and "HKS and HES". Kaos does not have any tracking detectors. In addition, Kaos has a thick Lead-Wall with a thickness of more than 10 cm to suppress the positron background from the target. Uncertainty of the flight path length to the target due to the multiple scattering effects in the lead wall makes the coincidence time resolution worse (∼1.5 ns in rms). Since HKS has drift chambers and no thick material from the target to the tracking detector, good coincidence time resolution is achievable. In the previous $(e, e'K^+)$ experiments, beam bunch structure could find clearly.

- Better hypernuclear yield
  The energy threshold of Λ production is 911 MeV. Virtual photons (VP) around the Λ threshold can only use in the MAMI experiment. A much wider VP energy region is available in the proposed experiment because the beam energy is 2.24 GeV, in which the energy region produces Λs effectively (Figure 14).

The expected setup parameters are listed in Figure 4. More hypernuclei production yield is available thanks to the higher beam energy. Though K^+ tagger PCS+HKS has a less solid angle and longer flight path length than Kaos, K^+ ID performance has much better. π^- spectrometer Enge has a tiny solid angle. Higher beam energy and K^+ ID performance can compensate for this demerit.

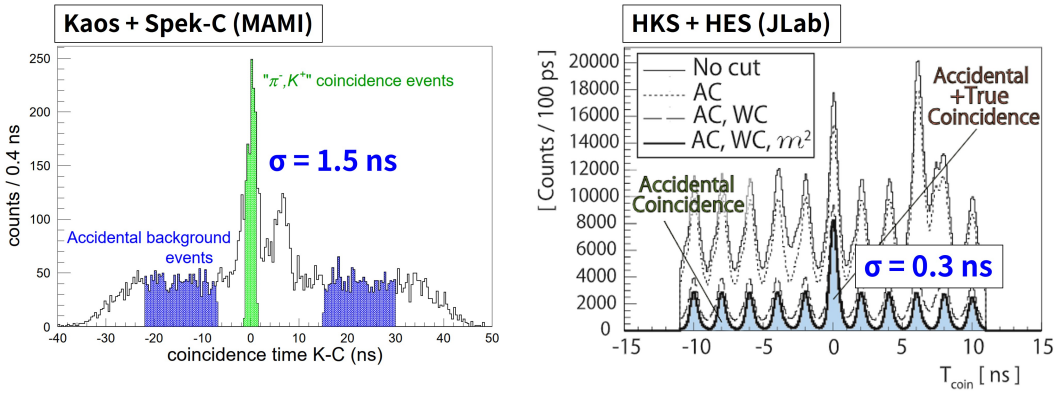

Figure 13: Coincidence time distribution. Coincidence time between Kaos and Spek-C at MAMI (Left). Coincidence time between HKS and HES at JLab E05-115 [5] (Right).

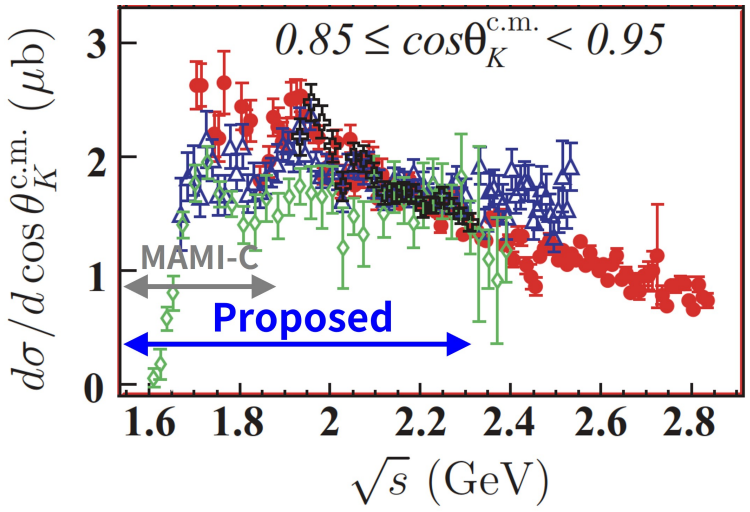

Figure 14: Differential cross-section of the (γ, K^+) reaction [24]. Energy coverage of the MAMI experiments and the proposed experiments are shown.

Table 4: Kinematic parameters of the MAMI experiment and the proposed experiment.

		MAMI	Proposed
Beam	Energy (GeV)	1.508	2.24
K^+ Tagger	Spectrometer	Kaos	PCS + HKS
	K^+ Angle (deg)	0	8
	Solid Angle (msr)	17	8.3
	Path Length (m)	6.4	11
π^- Spec.	Spectrometer	Spek-C	Enge
	π^- Angle (deg)	126	135
	solid Angle (msr)	28	4
	Mom. Resolution ($\Delta p/p$)	1×10^{-4}	3×10^{-4}
	Path Length (m)	10.75	5
Others	Mom. Transfer (MeV/c)	400	400

4.2 Estimation

An expected yield of hypernuclei is obtained as,

$$N_{HYP} = N_\Lambda \, R_{F.P} \, R_{stop} \, \Gamma_{\pi^-} \, \Delta\Omega_{\pi^-} \, \varepsilon_{\pi^-}^{decay} \, \varepsilon_{\pi^-}^{det} \ , \tag{5}$$

where

$$\begin{aligned}
N_\Lambda &: \text{The number of } \Lambda \text{ hyperons with } \mathrm{K}^+ \text{ tagging,} \\
R_{F.P} &: \text{Hyperfragment formation probability,} \\
R_{stop} &: \text{Hyperfragment stopping probability in target,} \\
\Gamma_{\pi^-} &: \frac{\Gamma(\mathrm{X}+\pi^-)}{\Gamma_{all}}, \text{ Branching ratio of } {}^{\mathrm{A}}_{\Lambda}\mathrm{Z} \rightarrow \pi^- + {}^{\mathrm{A}}(\mathrm{Z}+1), \\
\Delta\Omega_{\pi^-} &: \text{Solid angle of } \pi^- \text{ spectrometer,} \\
\varepsilon_{\pi^-}^{decay} &: \text{Survival ratio of } \pi^-, \\
\varepsilon_{\pi^-}^{det} &: \text{Detection efficiency of } \pi^-.
\end{aligned}$$

N_Λ is represented as follows:

$$N_\Lambda = N_{\gamma^*} \, N_t \frac{d\sigma_\Lambda}{d\Omega} \, A^{0.8} \Delta\Omega_{K^+} \, \varepsilon_{K^+}^{decay} \, \varepsilon_{K^+}^{det}, \tag{6}$$

where

$$\begin{aligned}
N_{\gamma^*} &: \text{The number of virtual photons associated with } \Lambda \text{ production,} \\
N_t &: \text{The number of atoms in production target,} \\
\frac{d\sigma_\Lambda}{d\Omega} &: \text{Differencial cross section of } (\gamma^* + \mathrm{p} \rightarrow K^+ + \Lambda), \\
A &: \text{Mass number of target nucleus,} \\
\Delta\Omega_{K^+} &: \text{Solid angle of } K^+ \text{ tagger,} \\
\varepsilon_{K^+}^{decay} &: \text{Survival ratio of } K^+, \\
\varepsilon_{K^+}^{det} &: \text{Detection efficiency of } K^+.
\end{aligned}$$

N_{γ^*} is described by,

$$\begin{aligned}
N_{\gamma^*} &= N_e \, \Gamma_\gamma^{int}, & (7) \\
&= N_e \int_0^{4\pi} d\Omega \int_{E_{th}}^{E_{max}} d\omega \ \Gamma_\gamma(\theta, \omega). & (8)
\end{aligned}$$

where N_e is the number of beam electrons. Γ_γ^{int} is a virtual photon flux integrated by scattered electrons with a solid angle and an energy above Λ production threshold ($E_{th} = 0.911$ GeV), which can be estimated precisely. From the previous hypernuclear experiment E05-115 results, we know the Λ production yield is proportional to $A^{0.8}$. $d\sigma_\Lambda/d\Omega$ can be estimated precisely from the CLAS results and the model calculation about the $p(e, e'K^+)\Lambda$ reaction.

$R_{F.P}$ has an uncertainty because of the limited data. MAMI results mentioned $R_{F.P}$ of ${}^{4}_{\Lambda}\mathrm{H}$ is 1% for the ${}^{9}\mathrm{Be}$ target. Since $R_{F.P}$ has known A^{-2} dependence of the target nucleus

[23], one can assume $R_{F.P}$ of ${}^{4}_{\Lambda}$H. Recent emulation results suggest two-body decay pions from ${}^{3}_{\Lambda}$H is about 1/3 of that from ${}^{4}_{\Lambda}$H. $R_{F.P}$ of ${}^{3}_{\Lambda}$H can be estimated as well as that of ${}^{4}_{\Lambda}$H by using known Γ_{π^-}. $R_{F.P}$ would be pointed out a few tens % for ${}^{4}_{\Lambda}$H with the AMD calculation in Kawachi's thesis [25]. Therefore, reliable decay π^- yields of p-shell hypernuclei would be several to a few dozen %. The probability increases for the neutron-rich hypernuclei because $\pi^0 + n$ decay mode is suppressed, and $\pi^- + p$ mode is enhanced because n is already occupied in the daughter nucleus. Thus, $R_{F.P}$ can be assumed as a relative value from the $R_{F.P}$ of ${}^{4}_{\Lambda}$H from the ^{9}Be target.

Table 5 shows a summary of yield gain compared with the MAMI experiment. Thanks to the better K^+ trigger and DAQ system, it is possible to use a higher beam current and thicker target. The thicker target results in a higher hypernuclear stopping probability, which help us get a better yield. Thanks to the higher beam energy, the integrated virtual photon flux associated with K^+ production will be 4.7 times higher than the MAMI experiment. Since the momentum transfer in the reaction is similar to the MAMI experiment, similar formation probabilities of hyperfragments, which is about 1% for ${}^{4}_{\Lambda}$H, is expected. Though half of K^+ was absorbed in the lead-wall in the Kaos spectrometer, HKS does not have any lead-wall. The effect also improves the gain factor twice. Spek-C at MAMI is an excellent spectrometer with large solid angles and good momentum resolution. The gain factor of π^- spectrometer is only 0.23 by using the Enge magnet as a hardware spectrometer. However, more precise momentum calibration is possible in the off-beam condition because the calibration with α-sources is available. A better hypernuclear efficiency for the coincidence time cut is also expected in the proposed experiment. Thus, the total gain factor is more than 30 times. Since 37 counts of ${}^{4}_{\Lambda}$H were observed in 12 days at MAMI, about 600 counts of ${}^{4}_{\Lambda}$H can be expected only in 7 days in the proposed experiment for a ^{9}Be target.

Table 5: Hypernuclear yield gain (^{9}Be target).

Item		MAMI	JLab	Yield Gain
Kinematics	Beam Current (μA)	20	50	2.5
	Int. VP Flux (A.U.)	2.9	13.5	4.7
	Thickness (mg/cm^2)	39	150	3.7
	$^4_\Lambda$H Stop. Prob. (%)	42	81	1.9
	$^4_\Lambda$H Form. Prob. (%)	1	1	1.0
	Sub Total			**81**
K^+ Tagger	Solid Angle (msr)	17	8.3	0.49
	Survival Ratio (%)	40	30	0.74
	K^+ ID Eff. (%)	48	81	1.7
	Lead-wall Eff. (%)	50	100	2
	Sub Total			**1.2**
π^- Spec.	Solid Angle (msr)	28	4	0.14
	Survival Ratio (%)	32	51	1.6
	π^- ID Eff. (%)	90	90	1.0
	Sub Total			**0.23**
Others	CoinTime Eff. (%)	68	90	1.3
	DAQ Eff. (%)	87	90	1.0
Total				**31**

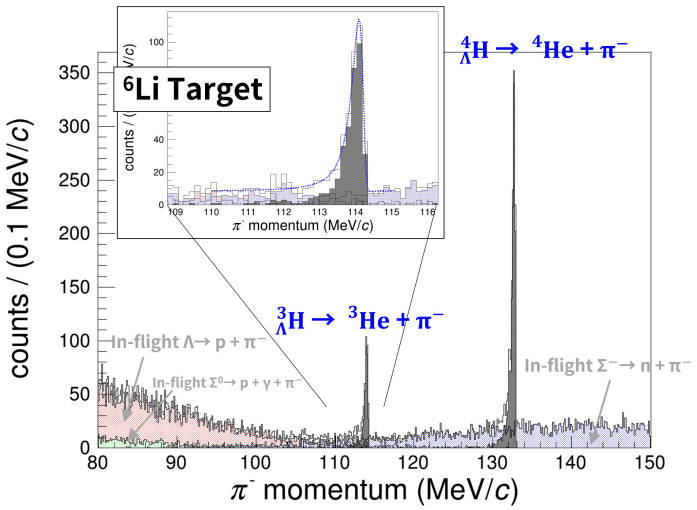

Figure 15: Pion spectrum of the Li target.

Table 6: Yield summary (^{6}Li target).

Hypernuclei	Form. Prob. $R_{F.P}$ (%)	Decay Branch Γ_{π^-} (%)	Yield (counts)
$^3_\Lambda$H	1.3	52	1300
$^4_\Lambda$H	2.4	29	400

4.3 Expected Results

This section shows expected decay pion spectra made by the Monte-Carlo simulation, including the reliable background distribution from quasi-free hyperons, the target energy struggling effect, and the spectrometer resolution.

4.3.1 Li target run

Figure 15 shows an expected spectrum with a ^{6}Li target in one week (168 hours) experiment. Possible hypernuclei and hyperfragments are only $^3_\Lambda$H and $^4_\Lambda$H on the π^- background from the in-flight hyperon decay. The peak width is 0.3 MeV/c in FWHM. The peak center can be determined with a precision of less than 1 keV for both hypernuclei. The precision is more than 10 times better than the world data.

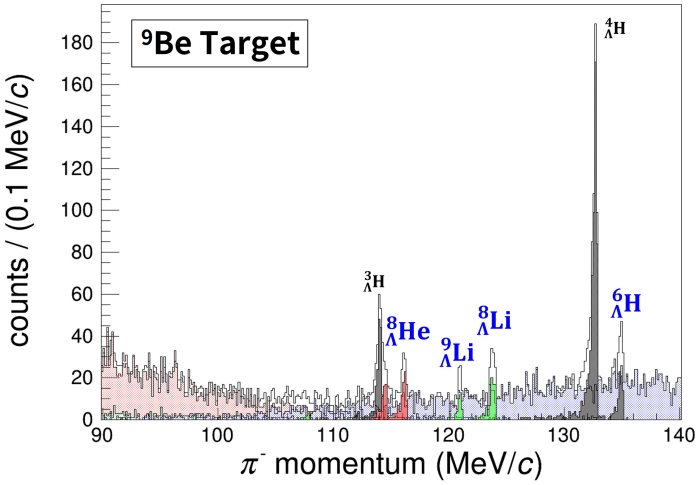

Figure 16: Pion spectrum of the Be target.

Table 7: Yield summary (^{9}Be target).

Hypernuclei	Form. Prob. $R_{F.P}$ (%)	Decay Branch Γ_{π^-} (%)	Yield (counts)
${}^{3}_{\Lambda}$H	0.6	29	180
${}^{4}_{\Lambda}$H	1.0	54	600
${}^{6}_{\Lambda}$H	0.3	30	100
${}^{8}_{\Lambda}$He	0.5	16	90
${}^{8}_{\Lambda}$Li	0.3	10	80
${}^{9}_{\Lambda}$Li	0.4	8	40

4.3.2 Be target run

Figure 16 shows an expected spectrum with a ^{9}Be target in one week (168 hours) experiment. Possible hypernuclei and hyperfragments are listed in Table 7. A few hypernuclei are expected around 120 MeV/c. The statistical error of the peak center is 10 keV/c for ${}^{8}_{\Lambda}$He, for example. ${}^{8}_{\Lambda}$He is one of the crucial hypernuclei to evaluate ΛN-ΣN coupling effect, though the latest Λ binding energy is quite large ($B_{\Lambda} = 7.16 \pm 0.70$ MeV). The existence of ${}^{6}_{\Lambda}$H is under discussion. The ${}^{6}_{\Lambda}$H peak can be identify if it is in a bound state because the expected peak position is isolated.

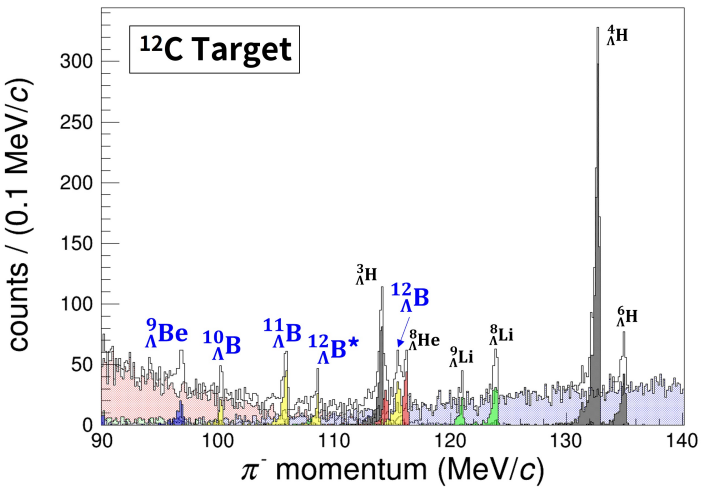

Figure 17: Pion spectrum of the C target.

Table 8: Yield summary (^{12}Be target).

Hypernuclei	Form. Prob. $R_{F.P}$ (%)	Decay Branch Γ_{π^-} (%)	Yield (counts)
$^{3}_{\Lambda}$H	0.3	29	320
$^{4}_{\Lambda}$H	0.5	52	1100
$^{6}_{\Lambda}$H	0.2	30	180
$^{8}_{\Lambda}$He	0.3	16	160
$^{8}_{\Lambda}$Li	0.2	10	150
$^{9}_{\Lambda}$Li	0.2	8	70
$^{9}_{\Lambda}$Be	0.2	8	80
$^{10}_{\Lambda}$B	0.1	18	70
$^{11}_{\Lambda}$B	0.2	18	180
$^{12}_{\Lambda}$B	0.4	20	200

4.3.3 C target run

Figure 17 shows an expected spectrum with a ^{12}C target in three weeks (504 hours) experiment. Possible hypernuclei and hyperfragments are listed in Table 8. Additional peaks from $^{9}_{\Lambda}$Be and $^{10,11,12}_{\Lambda}$B hypernuclei can be expected more than 5σ significance. One of the unique pion peaks comes from $^{12}_{\Lambda}$B. Two pion peaks, which are $^{12}_{\Lambda}$B$\rightarrow^{12}$B(0^+, g.s) $+\pi^-$ and $^{12}_{\Lambda}$B$\rightarrow^{12}$B(2^+) $+\pi^-$, are expected depending on the Spin state of $^{12}_{\Lambda}$B. The C target run is one of the most exciting runs in the proposal.

4.3.4 Al, Ca, and Pb target runs

In the larger atomic mass target, many kinds of hyperfragments from the s-shell to heavy atomic mass would be generated. The Pauli blocking principle suppresses MWD mode; observation of decay pion peaks from heavy hypernuclei might be difficult. However, the decay pion peak measurements of p-shell and sd-shell hypernuclei still have a chance. In addition, a target mass dependence of hyper-fragment formation probabilities, which nobody knows the such mass region, can be measured by using these targets without any risks.

4.3.5 Requested beamtime summary

In the proposed experiment, almost of all beamtime is shared by the $(e, e'K^+)$ experiment (E12-15-008 and E12-20-013) and the other hypernuclear LoI. Getting decay pion spectra is possible without additional beamtime requests for Li, Be, B, Al, Ca, and Pb targets. Though the C target run can expect many hypernuclear decay pion peaks, the hypernuclear yield is not enough to get in a week, which is the proposed $(e, e'K^+)$ experiment (E12-15-008) An additional two weeks (336 hours) beamtime for a C target is requested to get robust decay pion peaks.

5 Summary

Decay pion spectroscopy is a powerful technique to determine Λ binding energies of hypernuclear ground states. The experimental method was successfully established at MAMI. The proposed experiment will be a much higher statistics experiment using a high-quality CEBAF beam and have a chance to renovate current data of the light hypernuclei. The exact measurement can investigate (1) ΛN interaction, (2) Σ admixture effect from neutron-rich hypernuclei, (3) Resolving hypertriton puzzle, and (4) Hypernuclear Spin determination. Installing a third spectrometer, "Enge" in addition to the proposed $(e, e'K^+)$ experiments, can be performed the project without any long beamtime requests.

References

[1] P. Eckert. Hypernuclear database. *https://hypernuclei.kph.uni-mainz.de/.*

[2] C. Rappold *et al. Phys. Rev. C*, **88**:041001, 2013.

[3] M. Agnello *et al. Phys. Rev. Lett.*, **108**:042501, 2012.

[4] T. Miyoshi *et al. Phys. Rev. Lett.*, **90**:232502, 2003.

[5] T. Gogami *et al. Nucl. Inst. and Meth. A*, **900**:69, 2018.

[6] L. Tang *et al. Phys. Rev. C*, **90**:034320, 2014.

[7] A. Esser *et al. Phys. Rev. Lett.*, **114**:232501, 2014.

[8] T.O. Yamamoto *et al. Phys. Rev. Lett.*, **116**:222501, 2014.

[9] S.N. Nakamura *et al. Phys. Rev. Lett.*, **110**:012502, 2013.

[10] T. Gogami *et al. Phys. Rev. C*, **94**:021302, 2014.

[11] B.F. Gibson *et al. Phys. Rev. C*, **6**:741, 1972.

[12] Y. Akaishi *et al. Phys. Rev. Lett.*, **84**:3539, 2000.

[13] M. Juric *et al. Nuclear Physics B*, **52**:1, 1973.

[14] G. Keyes *et al. Nuclear Physics B*, **67**:269, 1973.

[15] J. Adam *et al. Phys. Lett. B*, **754**:360, 2016.

[16] L. Adamczyk *et al. Phys. Rev. C*, **97**:054909, 12018.

[17] J. Adam *et al. Nature Physics*, **16**:409, 2020.

[18] T. Motoba and K. Itonaga. *Prog. Theo. Phys. Supp.*, **117**:477, 1994.

[19] A. Gal. *Nucl. Phys. A*, **828**:72, 2004.

[20] M. Agnello *et al. Phys. Lett. B*, **681**:139, 2009.

[21] G. Audi *et al. Nucl. Phys. A*, **729**:337, 2003.

[22] J. Beringer *et al. Phys. Rev. D*, **86**:010001, 2012.

[23] H. Tamura *et al. Phys. Rev. C*, **40**:R479, 1989.

[24] M.E. McCracken *et al. Phys. Rev. C*, **81**:025201, 2010.

[25] A. Kawachi. Doctoral thesis. *University of Tokyo*, 1997.